Journal of Molecular Structure 920 (2009) 196–201

Contents lists available at ScienceDirect

Journal of Molecular Structure

journal homepage: www.elsevier.com/locate/molstruc

Synthesis, structures and temperature-induced phase transitions of the $Sr_2Cd_{1-x}Ca_xWO_6$ ($0 \leqslant x \leqslant 1$) double perovskite tungsten oxides

A. Faik [a,*], J.M. Igartua [a], J.L. Pizarro [b]

[a] Fisika Aplikatua II, Zientzia eta Teknologia Fakultatea, UPV/EHU, PB 644, Bilbao 48080, Spain
[b] Departamento de Mineralogía y Petrología, Facultad de Ciencia y Tecnología, UPV/EHU, PB 644, Bilbao 48080, Spain

ARTICLE INFO

Article history:
Received 2 September 2008
Received in revised form 24 October 2008
Accepted 27 October 2008
Available online 17 November 2008

Keywords:
Double perovskite
X-ray diffraction
Crystal structure
Phase transitions

ABSTRACT

The solid solution with double perovskite structure and general chemical formula $Sr_2Cd_{1-x}Ca_xWO_6$ ($0 \leqslant x \leqslant 1$) has been synthesized by the co-precipitation method. The Cd^{2+} cation substitution by Ca^{2+} in the Sr_2CdWO_6 double perovskite led to a continuous solid solution in the whole ($0 \leqslant x \leqslant 1$) fraction range. The crystal structures were determined from the Rietveld refinements of laboratory X-ray powder diffraction data. All members of the solid solution crystallize at room temperature in the $P2_1/n$ space group. The high-temperature study has revealed the following two phase-transition sequence for all the members of the solid solution: $P2_1/n \rightarrow I4/m \rightarrow Fm\bar{3}m$. The phase-transition temperatures of both successive phase-transitions showed a linear behavior in the whole ($0 \leqslant x \leqslant 1$) fraction range. Finally, following the results reported for Sr_2CdWO_6 and Sr_2CaWO_6, and comparing those temperatures with others of the Sr_2MWO_6 family reported previously, it was observed that the transition temperatures are higher in compounds with low tolerance factors.

1. Introduction

In recent years, compounds with general formula $A_2BB'O_6$ and double perovskite structure have been studied extensively since they present interesting and frequently unexpected magnetic and transport properties [1–3]. The $A_2BB'O_6$ double perovskite structure is derived from the ABO_3 simple perovskite structure when the octahedrally coordinated B-cations of the latter are occupied by two kinds of B and B′ cations with different charge and/or size. The ideal double perovskite structure has a cubic symmetry [4] with the $Fm\bar{3}m$ (No. 225) [5] space group. However, there are many factors (size – ionic radius – of the A-, B- and B′-site cations, different tilt-patterns of the BO_6 and $BB'O_6$ octahedra, among others) that lead to a reduction in the symmetry of the ideal structure giving rise, in the tungsten oxides, to monoclinic ($P2_1/n$, No. 14, non-standard setting) and/or tetragonal ($I4/m$, No. 87) symmetries. Also, in some double perovskite tungsten oxides, the monoclinic and tetragonal symmetries are converted to cubic at higher temperatures via one transition $I4/m \rightarrow Fm\bar{3}m$ [6,7] for the tetragonal phases; or two successive phase transitions: $P2_1/n \rightarrow I4/m \rightarrow Fm\bar{3}m$ [7,8], for the monoclinic ones.

In two previous works, we presented the experimental results, obtained by laboratory X-ray powder diffraction methods, for the crystal structures and the temperature-induced phase transitions in Sr_2CdWO_6 [8] and Sr_2CaWO_6 [7] ordered double perovskite tungsten oxides, the end-members of the solid solution analyzed in the present work. At room-temperature, the Cd- and Ca-containing compounds have the $P2_1/n$ space group; and, at high temperature both, too, show two successive phase transitions at 1105 and 1130 K, to the $I4/m$ space group tetragonal symmetry, respectively; and at 1223 and 1250 K, respectively, to the ideal $Fm\bar{3}m$ cubic symmetry.

In the study performed on Sr_2CdWO_6 [8], we also showed that there is a correlation between the tolerance factor [9] (in the end, controlled by the actual cation size) and (i) the temperature of the phase transitions and (ii) the extension in temperature of the monoclinically ($P2_1/n$ space group) and tetragonally ($I4/m$ space group) distorted phases observed in the Sr_2MWO_6 (M = Ni, Zn, Co, Mg, Cd, Ca) family.

The aim of the present work is to study the cation-size effect of the B-site (in the Sr_2BWO_6 ordered double perovskite structure) on the crystal structure of the $Sr_2\ Cd_{1-x}Ca_xWO_6$ solid solution, to understand how the double perovskite structure responds to changes in the effective size of the B-type cation. We will also explore the structural temperature-evolution of the members of the solid solution, to see how the cation-size effect is also present in the possible high-temperature phase transitions.

This is not the first time that solid solutions in compounds with double perovskite structure are analyzed. For instance, in [10–12] the authors explore the A-site cation-size effects on the possible appearance of phase transitions, and in [13,14], the B-site cation-size effect is studied. In all the cases though, only the room-temperature phases and cation substitution induced phase transitions

* Corresponding author. Tel.: +34 695741545; fax: +34 946013500.
E-mail address: abdessamad.faik@ehu.es (A. Faik).

0022-2860/$ - see front matter © 2008 Elsevier B.V. All rights reserved.
doi:10.1016/j.molstruc.2008.10.066

are studied. To the best of our knowledge this is the first time that the temperature evolution of the points in a solid solution of this kind is studied.

2. Experimental details

2.1. Sample preparation

The solid solution of $Sr_2Cd_{1-x}Ca_xWO_6$ was prepared in a series with x = 0.0, 0.2, 0.25, 0.4, 0.5, 0.6, 0.75, 0.8, 1.0 by the co-precipitation method. Stoichiometric quantities of $Sr(NO_3)_2$ (I), $Cd(NO_3)_2{\cdot}4H_2O$ (II), $Ca(OOCH_3)_2$ (III) and $(NH_4)_{10}W_{12}O_{41}$ (IV) were dissolved separately in distilled water. A slow addition, under magnetic agitation, of (IV) in (I and/or II + III) mixture at room-temperature induces the formation of a gelatinous precipitate. After evaporation at 60 °C, the resulting powder was progressively heated in air at 200 °C (12 h), 400°C (12 h), 600 °C (12 h), 900 °C (24 h) and 1000 °C (24 h). After each heating, the sample was cooled down slowly (3 K/min); and re-ground (re-mixed) to improve homogeneity. In order to control the quality of the obtained material, X-ray diffraction measurements were performed after each heating. For the x = 0.2, 0.8, 1.0 compositions, a single phase was obtained; and, for the rest of the compositions (x = 0.0, 0.4, 0.6), a small quantity ($\leqslant$3%) of $SrWO_4$ was found to be present as impurity (Fig. 1a).

2.2. X-ray powder diffraction

Diffraction data were collected at room-temperature on a Stoe STADI-P diffractometer equipped with a focusing germanium primary monochromator and a linear position-sensitive detector (PSD). $CuK_{\alpha 1}$, λ = 1.5406 (Å), radiation was used. The data were collected over a range of 15–85° (2θ) with a step of 0.02°; the effective counting time was 10 s per step.

At high-temperature, powder diffraction data of conventional X-ray were obtained using a Philips X'Pert MPD System with CuK_α (Ni filter) radiation, equipped with a proportional detector. Intensity data were collected by continuous scanning with 2θ steps of 0.01°; and counting times of 12 s at each step. The Bragg-Brentano parafocusing geometry was used. An Anton Paar HTK16 temperature chamber was used with direct sample heating (Pt filament), with a temperature stability of 0.5 K, mounted on the same diffractometer. In the case of Sr_2CdWO_6, a Bruker D8 Advance θ/θ diffractometer was used; equipped with a Våntec high speed one-dimensional detector using CuK_α radiation and with an Anton Paar HTK2000 high-temperature chamber (Pt filament and a temperature stability of 0.5 K). Data were collected using continuous scan with steps of (2θ) steps of 0.0083° and total time per scan of 12 s.

The specimens for the high-temperature measurements were prepared by mixing the material under study with acetone. Then the mixture was 'painted' over the Pt-strip heater of the chamber. Special attention was paid to the additional peaks belonging to the Pt sample heater that are present in the high-temperature diffractograms, and that overlap with the peaks originating from the samples studied. These peaks were excluded from the refinement.

The Rietveld refinement of the structural models was performed using the WinPlotr/FullProf package [15]. The peak shape was described by a pseudo-Voigt function, and the background level was modeled using a polynomial function. The refined parameters were: background coefficients, scale factor, lattice constants, atomic positions, isotropic independent atomic displacement parameters, zero shift, peak profile and asymmetry parameters. The $SrWO_4$ impurity found to be present was included as secondary phase in the refinements.

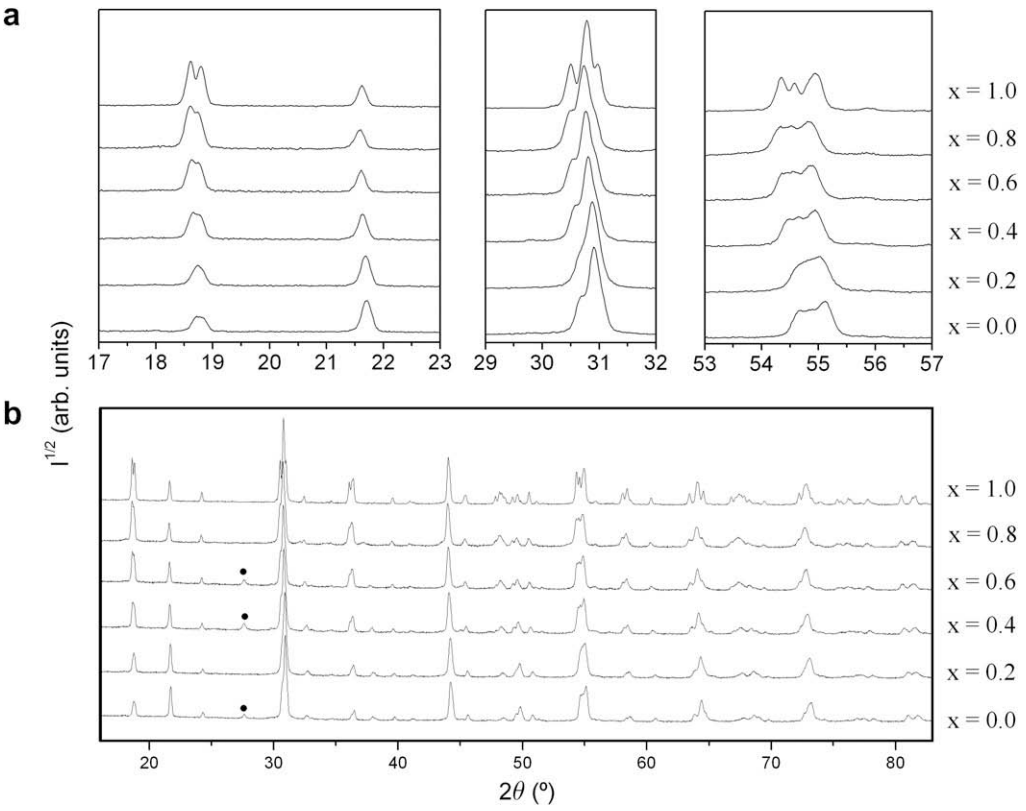

Fig. 1. (a) Evolution of the laboratory X-ray powder diffraction patterns of $Sr_2Cd_{1-x}Ca_xWO_6$: x = 0.0, 0.2, 0.4, 0.6, 0.8, 1.0. The bullet (•) indicates the small impurity, $SrWO_4$, only present in the x = 0.0, 0.4, 0.6 compositions. (b) Details from the X-ray powder diffraction patterns of $Sr_2Cd_{1-x}Ca_xWO_6$ (x = 0.0,0.2,0.4,0.6,0.8,1.0) in the 17–23°, 29–32° and 53–57° 2θ ranges, to show the continuous evolution of the patterns with the increasing Ca-content.

3. Results and discussion

3.1. Room-temperature structures

Fig. 1a shows the room-temperature X-ray powder diffraction patterns for the various compositions of $Sr_2Cd_{1-x}Ca_x WO_6$, in the 17–82° 2θ range. Based on a visual inspection of the room-temperature X-ray powder diffractograms (Fig. 1b), as there is a continuous change in the position of the peaks and in their form, evolving from the Cd-containing compound to the Ca-containing one, it is clear that the substitution of the Cd cation by Ca gives rise to a continuous solid solution: all the compositions are in a double perovskite phase with good homogeneity. As mentioned, the end-members of this solid solution crystallize, at room-temperature, in a monoclinic symmetry ($P2_1/n$) [7,8]. Thus, we expected that the members of the solid solution also crystallize in the same space group. Indeed, for all the studied compositions, all the reflections in each diffractograms, could be indexed in the $P2_1/n$ space group. We performed two sets of refinements: in the first one, we used the room-temperature structure of Sr_2CdWO_6 as the starting model; in the second one, we used the room-temperature structure of Sr_2CaWO_6. In both cases we obtained the same refined structural model for each of the solid solution members.

As a representative, in Fig. 2, we show the results of the refinements for the $x = 0.2$ composition. For all phases we obtained a good agreement between the experimental and the calculated diffraction profiles. Table 1 summarizes the room-temperature unit-cell parameters, atomic positions and isotropic independent atomic displacement parameters and the reliability factors of the Rietveld refinements for the studied compositions; except for the $x = 0.25, 0.50, 0.75$ values, not to overload the table. In these refinements, the atomic positions and unit-cell parameters of Sr_2CdWO_6 and Sr_2CaWO_6 are very close to those found in our recent works [7,8]. The small differences are attributed to the different methods of preparation (co-precipitation method for the materials of this work, and solid state method for the materials of our recent works) and to the different experimental equipments used.

Fig. 3 shows the (a) *a*, *b* and *c* lattice parameters, (b) monoclinic angle (β) and the (c) unit-cell volume of the synthesized materials. All those parameters increase linearly with the Ca amount, a clear evidence that the Vegard's law holds for this solid solution.

3.2. High-temperature structures and phase transitions

As the room-temperature results indicated that Vegard's law holds, for the high-temperature study we analyzed only three compositions, $x = 0.25$, 0.50, 0.75. For the high-temperature phase-transitions search, we have chosen two 2θ regions: the first one centered at about 24°, and the second one, depending on the material, between 71.0 and 74.0°. At all temperatures covered, these regions contain a group of diffraction peaks that have been identified as especially sensitive to the structural changes occurring in double perovskite materials [8]. These experiments showed that, in the low-angle interval, the peak disappears at a certain temperature; and the only changes that can be interpreted as indications of phase transitions, in the high-angle interval, are the appearance of a very weak shoulder on the low-angle side of the peak (in coincidence with the disappearance of the peak in the low-angle interval); and the subsequent unification of this shoulder with the main peak. Those changes were interpreted as evidences of the material undergoing two phase transitions; first, from the monoclinic structure to tetragonal one, and (at higher temperature) from tetragonal to cubic.

It should be noted that the diffraction experiments at the highest measured temperatures show that the weight fraction of $SrWO_4$ increases, indicating partial decomposition of the sample. This fact has also been clearly observed in Sr_2CdWO_6 [8].

The peak present in the low-angle interval, in all the materials of the solid solution (Fig. 4), is of the type $h + k + l = 2n + 1$, and disappears, which means that the there is a change from a primitive

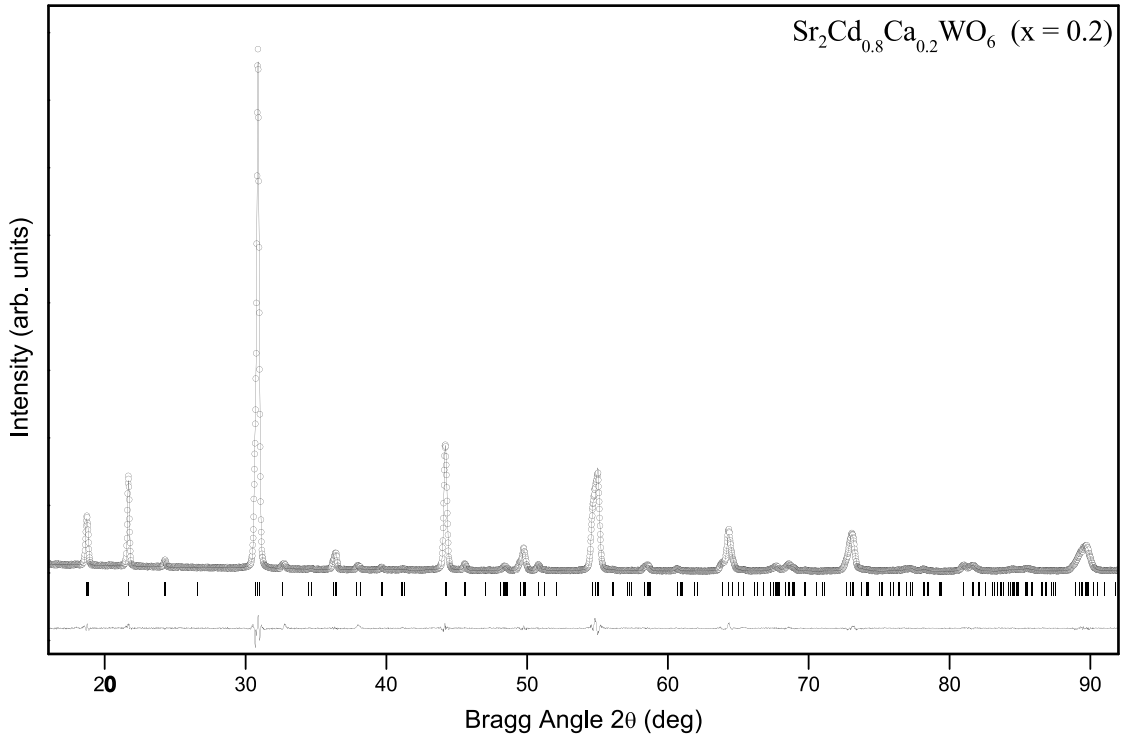

Fig. 2. Observed (·), calculated (–) and difference profiles for the Rietveld refinements of $Sr_2Cd_{1-x}Ca_xWO_6$ ($x = 0.2$), at room-temperature, space group $P2_1/n$.

Table 1
Refined structural parameters for the $Sr_2Cd_{1-x}Ca_xWO_6$ solid solution, at room-temperature, as a function of calcium content (x = 0.0, 0.2, 0.4, 0.6, 0.8, 1.0). The atomic positions (in fractional coordinates) and the isotropic independent atomic displacement parameters were refined in the space group $P2_1/n$. W atoms occupy the site 2a (0, 0, 0); and Cd and/or Ca occupy the site 2b ($\frac{1}{2}, \frac{1}{2}, 0$). O and Sr atoms occupy the site 4e (x, y, z).

Composition		x = 0	x = 0.2	x = 0.4	x = 0.6	x = 0.8	x = 1
Sr	x	0.0090(9)	0.0065(2)	0.0110(9)	0.0098(8)	0.0088(7)	0.0091(3)
	y	0.5362(2)	0.5356(2)	0.5374(3)	0.5380(2)	0.5362(3)	0.5391(2)
	z	0.2513(4)	0.2519(4)	0.2509(4)	0.2513(3)	0.2517(3)	0.2506(2)
O1	x	−0.087(2)	−0.080(3)	−0.077(3)	−0. 078(2)	−0.089(2)	−0.082(1)
	y	−0.025(2)	−0.014(2)	−0.017(2)	−0. 018(2)	−0.026(2)	−0.023(1)
	z	0.221(2)	0.223(3)	0.223(2)	0.221(2)	0.224(2)	0.228(1)
O2	x	0.251(3)	0.270(3)	0.249(3)	0.248(3)	0.254(2)	0.269(1)
	y	−0.188(2)	−0.198(3)	−0.186(3)	−0. 191(2)	−0.175(2)	−0.1840(1)
	z	0.042(3)	0.036(2)	0.049(3)	0.051(3)	0.043(3)	0.039(2)
O3	x	0.190(2)	0.186(3)	0.188(3)	0.188(3)	0.183(2)	0.190(1)
	y	0.240(2)	0.243(2)	0.235(3)	0.239(2)	0.248(2)	0.264(1)
	z	0.054(3)	0.045(3)	0.058(3)	0.060(3)	0.051(2)	0.045(1)
B (Å^2)	W	0.11(3)	0.09(3)	0.33(4)	0.41(3)	0.09(3)	0.30(2)
	Ca,Cd	0.53(5)	0.21(5)	0.73(6)	1.03(6)	1.12(8)	0.69(6)
	Sr	0.69(3)	0.76(4)	0.22(4)	0.13(4)	0.51(4)	0.32(2)
	O1, O2, O3	0.47(16)	1.60(2)	0.65(2)	0.55(2)	0.50(2)	0.54(2)
Cell param.							
a (Å)		5.7594(2)	5.7682(3)	5.7747(2)	5.7809(2)	5.7839(3)	5.7867(7)
b (Å)		5.8209(2)	5.8296(2)	5.8426(3)	5.8531(3)	5.8592(3)	5.8688(9)
c (Å)		8.1663(3)	8.1762(4)	8.1939(4)	8.2067(4)	8.2133(4)	8.2193(2)
β (°)		90.040(1)	90.052(2)	90.076(6)	90.114(4)	90.140(3)	90.155(7)
V (Å^3)		273.91(6)	274.92(8)	276.46(4)	277.69(6)	278.28(4)	279.22(2)
Reliability fact.							
R_p (%)		8.02	8.72	10.30	10.50	9.86	6.95
R_{wp} (%)		9.28	10.40	12.10	11.30	11.60	8.36
R_{bragg} (%)		7.12	7.84	7.78	8.50	7.83	5.69
χ^2 (%)		1.70	1.77	2.41	1.78	2.18	2.16

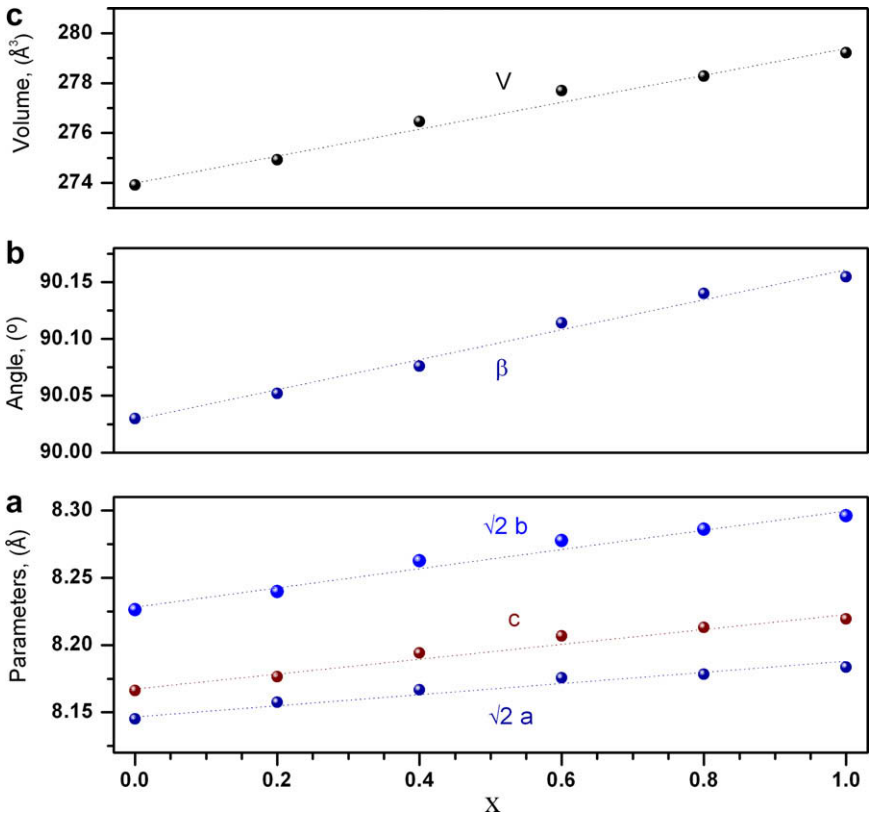

Fig. 3. Evolution, as a function of increasing calcium content, (x = 0, 0.2, 0.4, 0.6, 0.8, 1.0), at room-temperature, of the (a) unit-cell volume, (b) monoclinic angle (β) and the (c) unit-cell parameters of the synthesized materials. Dotted line is a guide for the eyes.

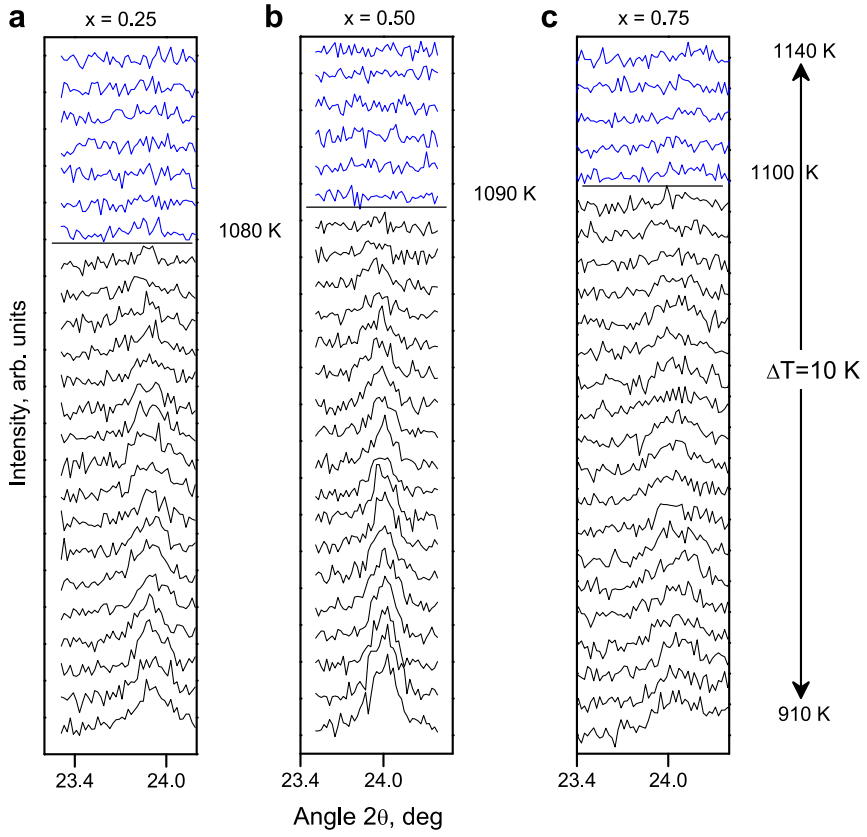

Fig. 4. Evolution with temperature and as a function of calcium content, (a) $x = 0.25$,(b) $x = 0.50$ and (c) $x = 0.75$, of the (1 1 1) and (−1 1 1) monoclinic reflections. Their disappearance marks the transition from a primitive cell ($P2_1/n$) to a centered one ($I4/m$). As the Ca content is increased, the temperature at which the transitions takes place also increases linearly: (a) $x = 0.25$, ≈1080 K, (b) $x = 0.50$, 1090 K and (c) $x = 0.75$, 1100 K.

unit cell to a body-centered one. Also, while some of the peaks remain split at those temperatures, others are well represented by a single diffraction reflection (Fig. 5). Analyzing the peak splitting, and taking into account the phase-transition sequence shown by the end-members of the solid solution, it becomes clear that at 1080, 1090 and 1100 K the unit cells of $Sr_2Cd_{1-x}Ca_x$ WO_6 ($x = 0.25$, 0.5, 0.75), respectively, are all tetragonal: $I4/m$ space group.

This tetragonal distortion gradually disappears at higher temperature, and suggests that at the highest measured temperatures, the unit cells are converted to cubic. This cubic phase most probably has the symmetry of the aristotype double perovskite structure with space group $Fm\bar{3}m$. This is the result we obtained for the Ca containing compound, and this is what we suggested for the Cd-containing compound.

For the case of the monoclinic-to-tetragonal phase transition we have assigned the first temperature at which the (−1 1 1) and (1 1 1) reflections are absent (Fig. 4) and the left shoulder (which is indicated by arrows in Fig. 5(b)) is observed. For the tetragonal-to-cubic ones, the first temperature at which the mentioned left shoulder disappears. The temperatures assigned to the successive phase transitions, at the measured compositions, are included in the corresponding panels in Fig. 5.

The structural analysis based on the presented temperature-dependent conventional diffraction experiments suggests that the phase-transition sequence existing in the continuous Sr_2Cd_{1-x}

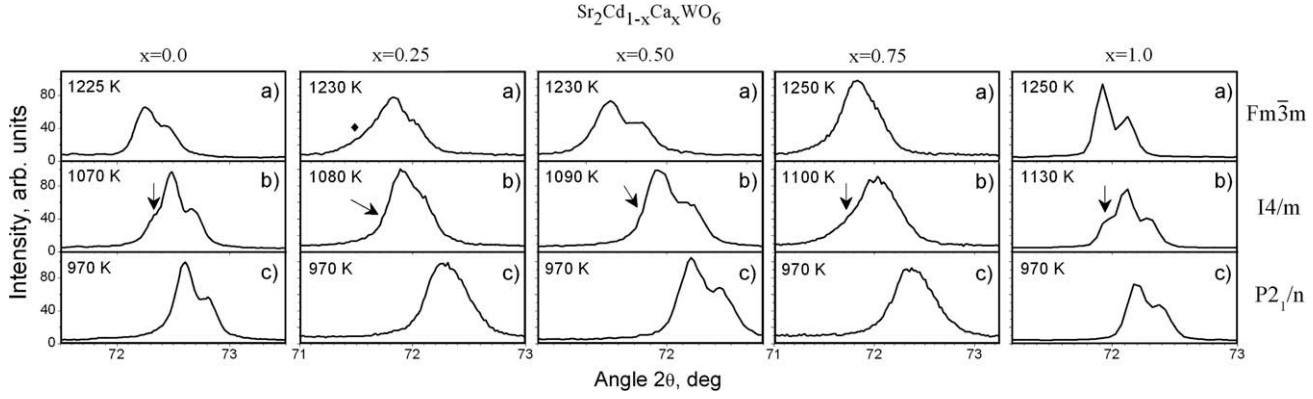

Fig. 5. Evolution with temperature and as a function of calcium content, of the (620) cubic reflection, (a) The tetragonal distortion, (b) is evidenced by the appearance of a weak shoulder at the left side of the reflection, indicated by the arrow. Finally, in the (c) the monoclinic distortion is shown. The bullet in the $x = 0.25$ Ca fraction content, in the (a) indicates the shoulder attributed to the formation of the $SrWO_4$ impurity as the sample decomposes at high temperature.

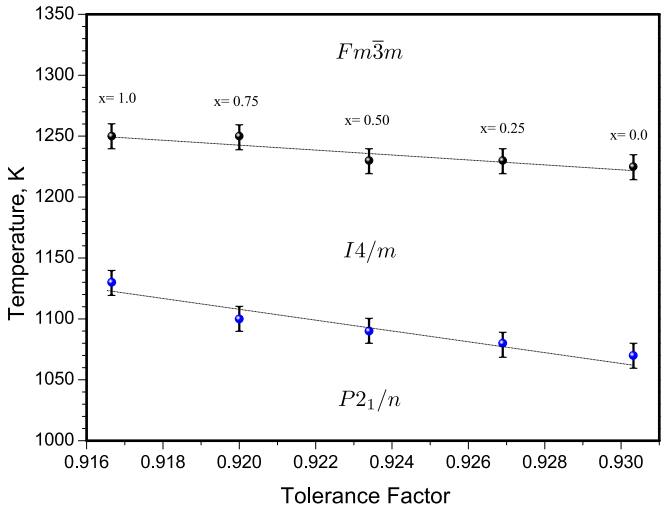

Fig. 6. Phase-transition temperatures of the successive phase transitions of the $Sr_2Cd_{1-x}Ca_xWO_6$ solid solution, as a function of their respective tolerance factors at room-temperature. Continuous line is a guide for the eyes.

Ca_xWO_6 ($0 \leqslant x \leqslant 1$) solid solution is $P2_1/n \rightarrow I4/m \rightarrow Fm\bar{3}m$. As we pointed out in [8], the same phase-transition sequence is observed in the Sr_2BWO_6 double perovskite oxide family, suggesting that the temperature evolution of their structures is governed by the same principles.

It is usually assumed [16] that the driving force of the structural changes in this kind of materials is the mismatch between the size of the A cation (Sr^{2+} in this case) and the interstitial space between the BO_6 and $B'O_6$ octahedra. This mismatch is measured by means of the so-called tolerance factor [9]: $t = \sqrt{2}\frac{d_{A-O}}{(d_{B-O}+d_{B'-O})}$. In the present case, $d_{B-O} = (1-x)d_{Cd-O} + x\ d_{Ca-O}$. We have obtained the mean d_{Sr-O}, d_{Cd-O}, d_{Ca-O} and d_{W-O} bond lengths by calculating the room-temperature distances that give the nominal oxidation states of the cations in the bond-valence method [8,17]. In Fig. 6 we show the phase-transition temperatures of the successive phase transitions as a function of the tolerance factor t at room-temperature.

A clear linear behavior of the cubic-to-tetragonal phase-transition temperature is observed, in accordance with the result obtained for the whole Sr_2BWO_6 (B = Ca, Cd, Mn, Zn, Mg, Co, Cu, Ni) family [6–8]. The same is true for the tetragonal-to-monoclinic transition, if the value for that phase transition in $Sr_2\ CdWO_6$ is revisited [8]. The actual temperature (1070 K) for the tetragonal-to-monoclinic transition in Sr_2CdWO_6, belonging to the preparation presented in this work, is a slightly lower than the previously reported one (1105 K) [8] in a sample from another preparation, measured in another equipment, and that showed, at high-temperatures, a progressive decomposition which could be responsible for a slightly different stoichiometry, affecting the symmetry, and, in turn, influencing in the temperature value for the phase transition.

These results confirm that the most important factor governing the appearance of octahedral tilts in the double perovskite structure and the temperature range in which they exist is a geometrical one: the mismatch between the size of the A cation and interstitial space between the BO_6 and $B'O_6$ octahedra, irrespective of having a solid solution in the B-site, at least for the studied solid solution.

4. Conclusions

The Cd^{2+} cation progressive substitution by Ca^{2+} in the Sr_2CdWO_6 double perovskite led to a continuous solid solution in the whole ($0 \leqslant x \leqslant 1$) fraction range. The crystal structures, at room-temperature, of all the members of the solid solution were determined from the Rietveld refinements of laboratory X-ray powder diffraction data: they crystallize in the $P2_1/n$ space group. The high-temperature study revealed the following two phase-transition sequence, for all the members of the solid solution: $P2_1/n \rightarrow I4/m \rightarrow Fm\bar{3}m$. The cation substitution does not induce a phase transition, and the phase-transition sequence observed in the end members of the solid solution is also observed in the solid solution. The phase-transition temperatures of both successive phase-transitions showed a linear behavior in the whole ($0 \leqslant x \leqslant 1$) fraction range. It was observed that the transition temperatures are higher in compounds with low tolerance factors, as in the case of the members of the Sr_2MWO_6 family.

Acknowledgements

We thank Dr. Gateshki for the very helpful discussions during the preparation of the manuscript. This work was done in part under project numbers: UPV 0063.310-13564/2001-2006 and FIS2005-07090. The authors thank the technician of SGIker, Dr. J. P. Chapman, financed by the Programa Nacional de Potenciación de Recursos Humanos del Plan Nacional de Investigación Científica, Desarrollo e Innovación, Ministerio de Ciencia y Tecnología y Fondo Social Europeo (FSE), for the X-ray diffraction.

References

[1] K.-I. Kobayashi, T. Kimura, H. Sawada, K. Terakura, Y. Tokura, Nature 395 (1998) 677–680.
[2] M. DeMarco, H.A. Blackstead, J.D. Dow, M.K. Wu, D.Y. Chen, E.Z. Chien, H. Haka, S. Toorongian, J. Fridmann, Phys. Rev. B 62 (2000) 14301–14303.
[3] Y. Todate, J. Phys. Chem. Solids B 60 (1999) 1173.
[4] P.M. Woodward, Acta Cryst. B53 (1997) 32.
[5] T. Hahn (Ed.), International Tables for Crystallography, vol. A, Kluwer, Dordrecht, 2002.
[6] M. Gateshki, J.M. Igartua, E. Hernández-Bocanegra, J. Phys. Condens. Matter 15 (2003) 6199–6217.
[7] M. Gateshki, J.M. Igartua, J. Phys. Condens. Matter 16 (2004) 6639–6649.
[8] M. Gateshki, J.M. Igartua, A. Faik, J. Solid State Chem. 180 (2007) 2248–2255.
[9] V.M. Goldschmidt, Str. Nor. Vidensk-Akad. Oslo 1 (1926) 1.
[10] Q. Zhou, B.J. Kennedy, C.J. Howard, M.M. Elcombe, A.J. Studer, Chem. Mater. 17 (2005) 5357–5365.
[11] Q. Zhou, B.J. Kennedy, M.M. Elcombe, Physica B Condens. Matter 385–386 (2006) 190–192.
[12] M.C.L. Cheah, B.J. Kennedy, R.L. Withers, M. Yonemura, T. Kamiyama, J. Solid State Chem. 179 (2006) 2487–2494.
[13] Q. Zhou, B.J. Kennedy, K.S. Wallwork, M.M. Elcombe, Y. Lee, T. Vogt, J. Solid State Chem. 178 (2005) 2282–2291.
[14] P.J. Saines, B.J. Kennedy, J. Solid State Chem. 181 (2008) 298–305.
[15] J. Rodríguez-Carvajal, Physica B 192 (1993) 55–69.
[16] N.E. Brese, M. O'Keeffe, Acta Cryst. B47 (1991) 192–197.
[17] Accumulated Table of Bond Valence Parameters Version 2.2 Prepared by I.D. Brown, McMaster University, Hamilton, Ontario, Canada. Available from: <www.ccp14.ac.uk/ccp/web-mirrors/i_d_brown>.